Deformation Studies of Aluminum Based High Strength Alloys-A New Approach

[1]Khalid Hussein Rahi, [2]Gopi Krishna

[1,2] Department Of Mechanical Engineering University College Of Engineering & Technology, Acharya Nagarjuna University Nagarjunanagar:: Guntur::Andhra Pradesh, 522 510a.P., India

Abstract: **There has been an increasing interest in composites containing low density and low cost reinforcements. So far most of the research work have been carried out by incorporating hard ceramic particles such as Al2O3, SiC, Flyash and graphite particles to soft matrix like pure aluminium A356, and many more alloys and very few worked on combination of reinforcements (hybrid composites). In the current work, an attempt has been made by combining two types of ceramic particles like flyash and silicon carbide in equal proportions for preparation of hybrid composites, which significantly improves the mechanical properties and wear properties of the Aluminum based MMCs.**

Experiments have been conducted under laboratory condition to assess the mechanical characteristics of the aluminium FA/and SiC composite under different size particle conditions. This has been possible by fabricating the samples through usual stir casting technique. To enhance the mechanical properties the surfaces of the samples were studied under optical microscope to get an idea about the effect of particulate reinforcement on the micro structure behavior of the composite. Dispersion of FA and SiC particles in aluminium matrix A356 improves the hardness of the matrix material and also the mechanical behavior of the composite.

Keywords: **Composites, Fabrication Facilities, Selection of Matrix Material, Fabrication and Characterization of Composites, Deformation Studies, Finite Element Simulation of Cold Upsetting Process.**

I. INTRODUCTION

1.1 COMPOSITES:

Composite is a system of materials, composing two or more materials mixed and bonded on a macroscopic scale. In general composite material consists of a reinforcement (fibers, particles, flakes, and/or fillers) embedded in a matrix (polymers, metals, or ceramics). The matrix holds a) the reinforcement to form the desired shape and, b) transfers the load to the reinforcement, while the reinforcement improves the overall mechanical properties of the matrix. The composite exhibits better properties than each constituent individual. Properties of composites are strongly dependent on the properties of their constituent materials, their distribution and interaction among them. [1].

1.2 CLASSIFICATION OF COMPOSITES:

In general, composites are classified according to the type of matrix material and the nature of reinforcement at two distinct levels. The first classification includes organic-matrix composites (OMCs), metal-matrix composites (MMCs) and ceramic-matrix composites (CMCs). The term “organic-matrix composite” is generally assumed to include two classes of composites: polymer-matrix composites (PMCs) and carbon-matrix composites [2].

The second classification refers to the reinforcement form particulate reinforcements, whiskers, continuous fibers, laminated composites, and woven composites. In order to provide a useful increase in properties, there must be a substantial volume fraction (10% or more) of the reinforcement. Reinforcement is considered to be a “particle” if all of its dimensions are roughly equal. Thus, particulate-reinforced composites include those reinforced by spheres, rods, flakes, and many other shapes of roughly equal axes. COMPOSITES can be classified into:

1. Polymer Matrix Composites (PMCs)

2. Ceramic Matrix Composites (CMCs)

3. Metal Matrix Composites

1.3 METAL-METAL COMPOSITES:

Applications of metal-ceramic composites are limited due to the non-compatibility between the matrix and reinforcement and lack of good interface among them. To limit the limitations associated with metal-ceramic composites, metal-metal composite systems were considered, where, two different metals; having good solubility one in the other, with uniform and compatible interface, when used as matrix and the reinforcement. The limited solubility led to the alloy formation passing solid solution strengthening while the undissolved particles help achieving dispersion strengthening. Madhu *et al*. [3] initiated this kind of works with aluminium-copper particulate systems.

1.4 AIM OF THE WORK:

Primary investigation is to devlop a metal-metal composite system to achieve improved mechanical properties and compare the behaviour with that of base alloy.

II. FABRICATION FACILITIES

2.1 Melting Furnace:

In the present investigation, preparation of alloys and fabrication of composites were carried out in pot furnace.

Figure 2.1 Pot furnace, with a stirrer

2.1.1 Secondary Processing:

Both alloy and composites were hot extruded using 200T press.

2. 2 TESTING FACILITIES:

A. Physical Testing:

1. Optical Microscopy

2. SEM and EDS

3. XRD

4. Melting Behaviour

5. Electrical Resistivity

6. Density and Porosity

B. Mechanical Testing:

1. Hardness:

Vickers microhardness studies were carried out for the investigated materials using vickers microhardness tester (Model: UHL IMS 4.0), and Leco vickers hardness tester (Model: LV 700, USA) with 1kg load. The indentation time for the hardness measurement was 15 seconds. An average of six readings was taken for each hardness value.

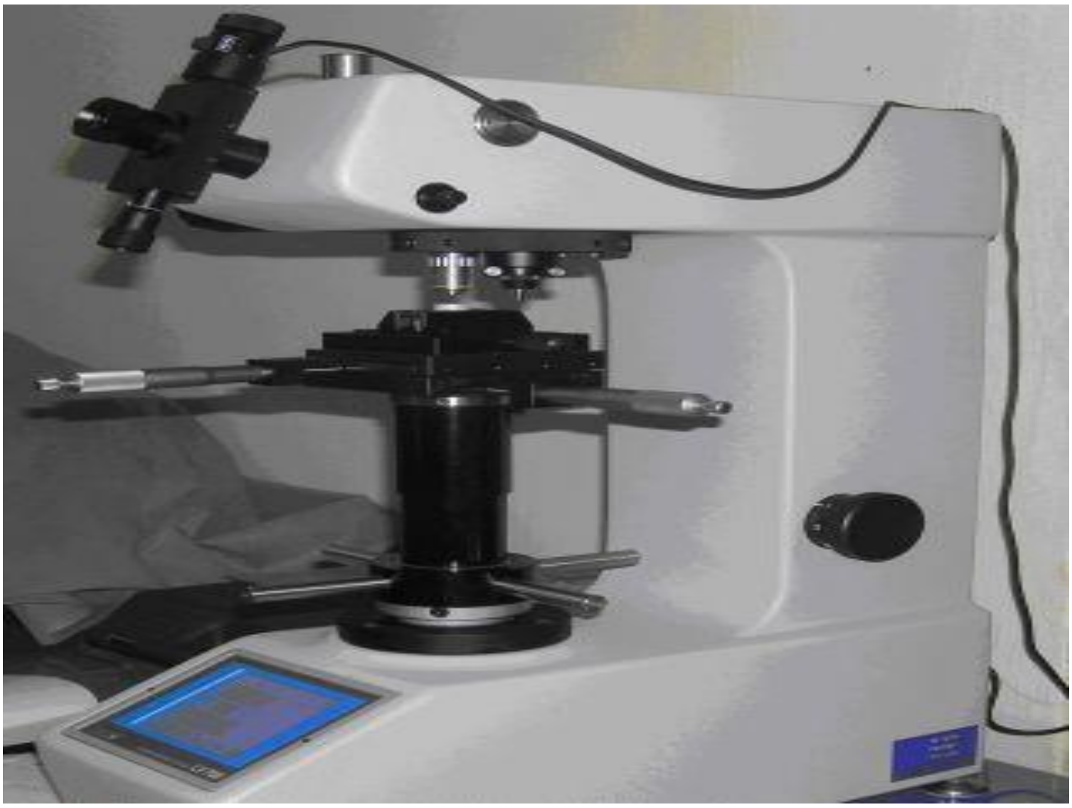

Figure 2.7 Leco (Model: LV 700, USA) Hardness tester

2. Tensile:

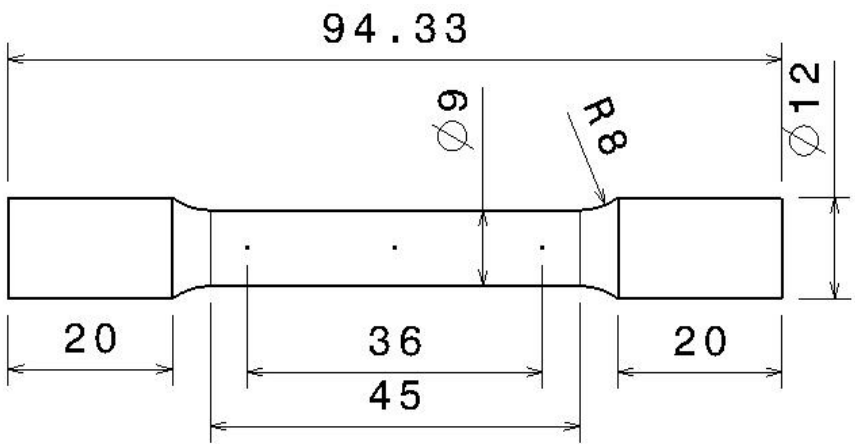

Figure 2.8 Geometry of specimen for tensile test

3. Compression

4. Ring Compression Test

III. SELECTION OF MATRIX MATERIAL

A356 -Al-Si is a binary alloy with 6.5% Si and small amounts of Cu, and other common elements. This alloy has a great importance in engineering industries, as it exhibit high strength to weight ratio, high wear resistance, low density, low coefficient of thermal expansion etc. Silicon imparts high fluidity and low shrinkage, which result in good castability, weldability. Presence of high hard silicon particles, improve wear resistance. The properties of casting alloy A356 are outlined in table 3.1 [4]. The Al-Si system, figure 3.1, has a eutectic reaction at 577ºC and a eutectic composition of 12.6 wt%. As aluminum and silicon solidify in different structures, respectively face centered cubic (FCC) and diamond cubic, two solid phases, α and β are produced. At high temperature, the hypoeutectic alloy forms a rich aluminum α- phase solid. The hypereutectic alloy forms almost pure β phase silicon. Very little silicon (1.65 wt%) dissolves in the α phase aluminum and almost negligible amount of aluminum dissolves in the β phase, figure 3.2 shows the microstructure of A356 alloy at 200x magnification.

Table 3.1: Properties of A356 casting alloy [1]

TensileStrength	221-262 Mpa
Yield Strength	165-185 Mpa
Elastic Modulus	72.4 GPa
Hardness	70-80 HB
Density	2.685Kg/m3
Liquidus Temperature	615ºC
Solidus Temperature	577ºC
Coefficient of Thermal Expansion	23.5μm/m•K at 20-300ºC
Thermal Conductivity at 25ºC	151-155W/m•K

Table 3.2: Chemical composition of A356 alloy, wt. %

Si	Mg	Cu	Ti	Zn	Fe	Al
6.5	0.4	0.05	0.06	0.03	0.09	Balance

3.2 SELECTION OF REINFORCEMENT MATERIAL:

Aluminium-Copper-Magnesium alloys were known for their high strength and stiffness. With a due advantage of high specific strength of these alloys, reinforcing in metal matrix composites (MMC's) yield better properties, find applications in aerospace, structural etc., at low cost. [5-7]

The prime idea of fabrication for a strong and wear resistant reinforcement, compatible with matrix material needs to be investigated for composite preparation. A series of alloys have been prepared and investigated for suitability as reinforcement.

3.3 PREPARATION OF BINARY AND TERNARY ALLOYS:

Figure 3.3 and 3.4 shows the process chart for the fabrication of Al-Cu binary and Al-Cu-Mg ternary alloys. Pure aluminium (cut pieces of ingot) melted in pot type electric resistance heating furnace, placing in clay graphite crucible at 700^0 C. Coverall, proprietary agent supplied by M/s Fosceco Ltd. was added (0.1 wt% of metal), at the start of melting to prevent oxidation. Copper was added to the melt at 700^0 C and increased the temperature of the melt to 850^0 C, maintained for one hour. After ensuring complete copper dissolution in the melt it was thoroughly mixed with a graphite sheathed tube for uniformity in composition. Temperature was reduced to 700^0 C. Magnesium in chip form wrapped in aluminium foil was added to the binary alloy, plunged to bottom of the melt for complete dissolution and prevent oxidation. Melt was well mixed with a graphite sheathed tube for uniformity in composition. Once again a small amount of coverall was added to the melt. Metal was thoroughly degassed using Argon for one minute at the pouring temperature. After skimming off the oxidized layer, metal was cast into 170 mm x 18mm Ø finger moulds.

International Journal of Mechanical and Industrial Technology ISSN 2348-7593 (Online)
Vol. 3, Issue 1, pp: (269-281), Month: April 2015 - September 2015, Available at: www.researchpublish.com

A series of Al–Cu binary and Al-Cu-Mg ternary alloys were produced with copper ranged from 10 to 20% by weight for binary alloys (Al-10Cu and Al-20Cu); 10%Mg and 20%Mg by weight for ternary alloys (Al-10Cu-10Mg, Al-10Cu-20Mg, Al-20Cu-10Mg, Al-20Cu-20Mg). Cast ingots, figure 3.5, were homogenized at 100°C for 24 hrs.

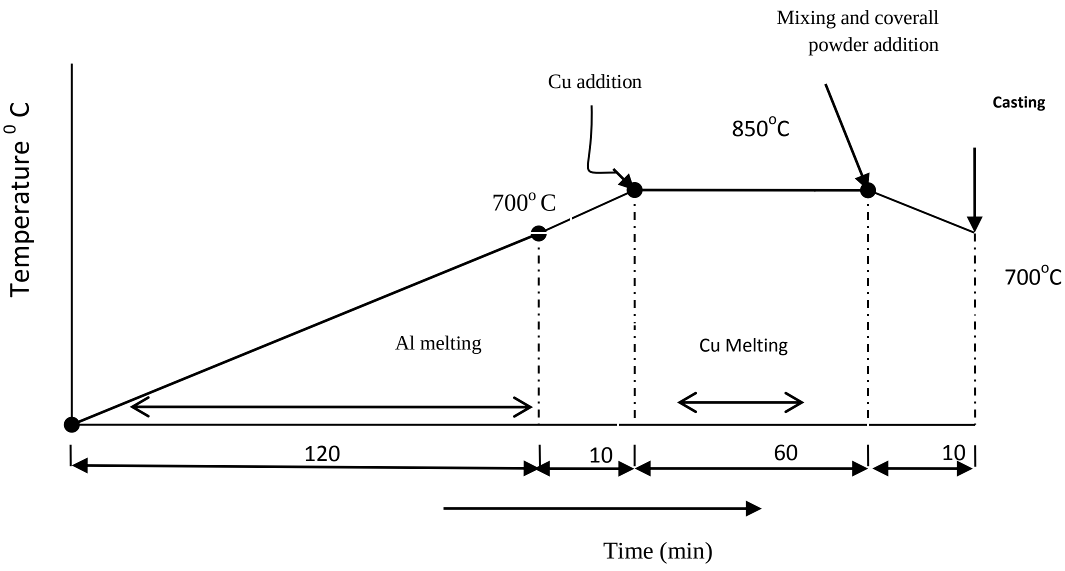

Figure 3.3 Process chart for preparation of binary alloys

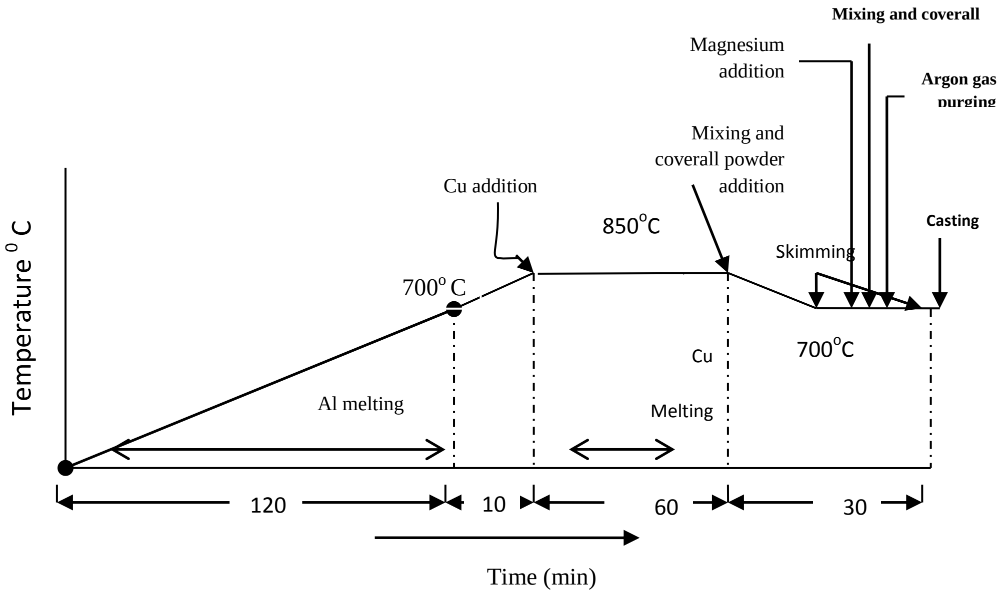

Figure 3.4 Process chart for preparation of ternary alloys

Table 3.3 Chemical composition of the binary and ternary alloys (in wt. %)

Material	Elements									
	Cu	Mg	Si	Fe	Mn	Ni	Pb	Sn	Ti	Zn	Al
Al-10Cu	9.12	-	0.038	0.562	0.123	0.068	-	-	0.011	0.12	Bal.
Al-20Cu	18.98	-	0.042	0.468	0.189	0.091	0.025	0.05	0.048	0.035	Bal.
Al-10Cu-10Mg	8.92	7.72	0.192	0.76	0.212	0.086	-	0.014	0.021	0.14	Bal.
Al-20Cu-10Mg	19.32	8.89	0.125	0.67	0.129	0.068	0.032	-	0.018	0.13	Bal.
Al-10Cu-20Mg	9.2	19.01	0.21	0.81	0.11	0.056	0.29	0.054	-	0.31	Bal.
Al-20Cu-20Mg	19.15	18.89	0.29	0.91	0.04	0.054	0.02	0.48	-	0.17	Bal.

3.7 SELECTION OF REINFORCEMENT SIZE:

3.7.1 Production of Powders:

Alloy powders are produced by different techniques depending on the application involved. In the present investigation, Al-Cu-Mg alloy powders were produced by filing techniques, where, fingers rotating on a lathe, figure 3.13, were filed with speeds of rotation ranging between 800, 480 and 290 rpm and files. Finer powders were obtained at high speed and with finer files.

3.7.2 Characterization of Powders:

3.7.2.1 Alloy Powders:

Figure 3.14 shows the filings of particulate material. The average size was found to be between 200 and 300 µm. Further ball milling in a conventional ball mill for 1 hour, gave an average particle size of 125 µm with large fraction in -100, +120 mesh range. After thorough magnetization using a strong magnet, to remove the balls contamination, if any, the particulate material in the sieve range of -100 $_{+}$ 120 has been chosen for reinforcement purpose, shown in figure 3.15.

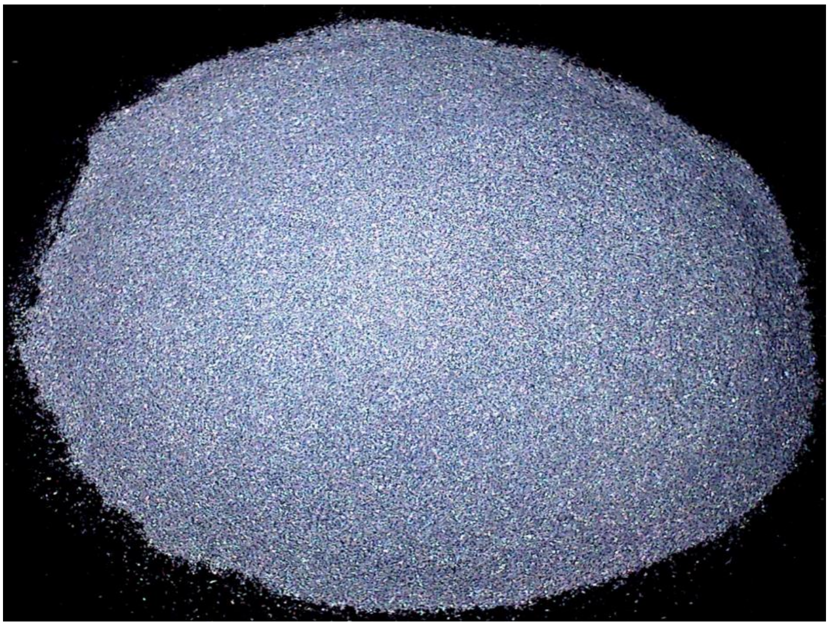

Figure 3.15 Powder with size 125-150 µm

3.8 CONCLUSIONS:

1. High hard, low resistivity alloy has been developed for the purpose of reinforcement applications.
2. High strength alloy particulate (HSA_p) reinforcement materials were prepared by filing and ball milling technique.

IV. FABRICATION AND CHARACTERIZATION OF COMPOSITES

4.1 INTRODUCTION:

Most of the investigations and research in MMCs, prioritized in increasing strength and hardness properties. Presence of hard and brittle reinforcements, restrict the mobility of dislocation, thus enhancing the strength properties. On the other hand, ductility decreases to a great extent, due to lack of interfacial bonding and fracture of reinforcements.

Fracture surface morphology of discontinuously reinforced metal matrix composites exhibit characteristic features of ductile rupture mechanism. This failure process can be conveniently split into three stages: void nucleation, growth and coalescence. Ductile fracture of monolithic alloys to the composites imply that the onset of void nucleation is the dominant process; controlling the ductility in these materials, with high volume fractions of reinforcement nucleation process to dominate, if void nucleation is at the reinforcing phase. Void growth and coalescence have been much neglected in the study of composites. Ductility of discontinuously reinforced metal matrix composites cannot be uniquely correlated with the void nucleation rate at the reinforcing particles.

4.2 EXPERIMENTAL WORK:

4.2.1 Fabrication of Composites

All the composites were synthesized through stir casting technique, which is a proven and well established method for composite (MMC) making. A356 alloy was melted in an electric resistance furnace. A temperature of 720^0 C, was maintained throughout

Interpretation: From the above table, it is observed that 50% the company have selection strategy Focus to fill the vacancies from within the company a large extent, 10% certain extent, 20% little extent and other 20% less extent. the process. The melt (1.5 kg) was thoroughly degassed using Argon, and gas jacket on melt was maintained throughout the process. A vortex was created at an rpm between 700 and 750 using a graphite impeller, preheated (200^OC) high strength alloy particulates ($HSA_{(P)}$) were added quickly (5-15 wt.%) and continuously to the vortex, through a screen. At the end the particulate addition, composite was cast into a cast iron cylindrical mould, figure 4.1. Hot ingot was transferred to a furnace at 100^OC, and homogenized for 24 hrs.

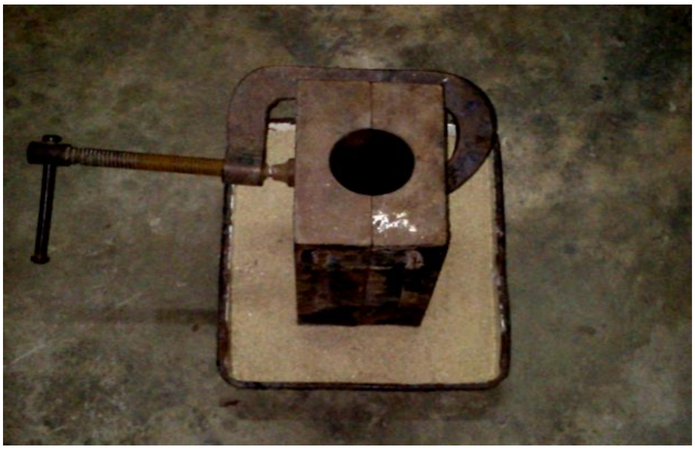

Figure 4.1) Die used for Composite preparation

4.2.2 Extrusion of Composites:

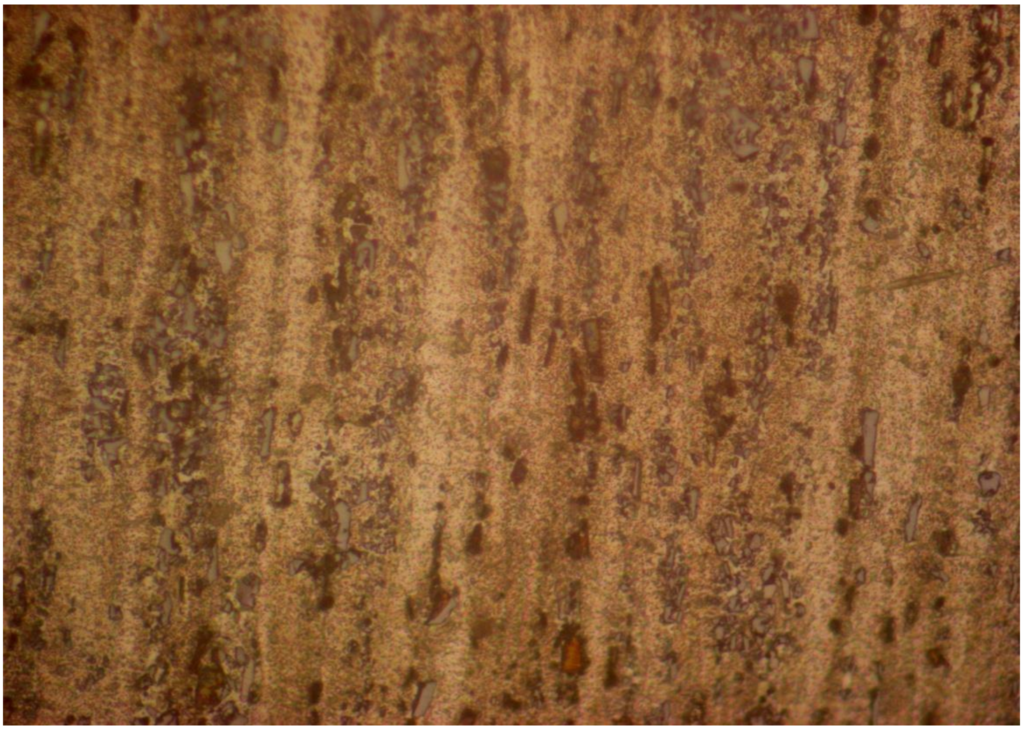

Figure 4.4 Microstructure of composite, showing banded particulates, 200 xs (Longitudinal direction)

4.3 RESULTS AND DISCUSSION:

It can be seen that, with increasing reinforcement content, the particle size is decreasing. An average of 50 readings was considered in each image, with over 20 SEM images for each composite. Few selected particles have been shown with magnified letters. Table 4.1 shows the average particle size of the reinforcement with increasing weight fraction. Since addition time for particulate material increases with increasing weight fraction, the particulates present in the molten metal for larger periods. Hence, there is surface dissolution in the matrix and correspondingly particulate size reduction is observed.

Table 4.1 Effect of particle size with the reinforcement

% of reinforcement	Size of particle (μm)	Surface area to volume ratio
5%	8.419 ± 0.42	0.7126
10%	4.825 ± 0.33	1.2435
15%	3.300 ± 0.33	1.8181

4.4 CONCLUSIONS:

1. Metal-Metal composites were fabricated by reinforcing High Strength Alloy Particulates ($HSA_{(P)}$) in A356 matrix.
2. Resultant composites were secondary processed by direct hot extrusion.
3. The decrease in particle size with increasing reinforcement content was due to increased casting time during processing.
4. Presence of reinforcement decreased the resistivity of the resultant composite
5. Composites exhibited improved hardness values compared to that of the alloy.
6. Increased reinforcement content enhanced the strength properties in terms of yield strength, ultimate tensile strength and modulus of elasticity.
7. The decrease in particle size caused

a. Enriched matrix concentration with Cu and Mg contents.

b. Enriched interfacial bond between the particulates and the matrix.

c. Fine grained structure due to increased nucleation phenomenon.

d. Enriched intermetallics contents.

e. Increased surface area to volume ratio of the reinforcement for cumulative effect of above.

V. DEFORMATION STUDIES

5.1 INTRODUCTION:

5.1.1 Upset Forging:

Many operations in manufacturing, particularly processes such as forging, rolling, and extrusion are performed with the workpiece subjected to compressive forces. The compression test, in which the specimen is subjected to a compressive load, gives information useful for these processes [8]. The test is usually carried out by compressing a solid cylindrical specimen between two flat dies. Upset forging or simple axial compression testing is useful for measurement of elastic and compressive fracture properties of both ductile and brittle materials. The true stress-true strain curves obtained from the compression test and tension tests on ductile materials coincide with each other, where as this does not hold true for brittle materials, which are generally stronger and more ductile in compression than in tension

5.1.2 True Stress and True Strain:

5.1.3 Engineering Stress and Engineering Strain:

5.1.4 Computation of Plastic Strain:

5.2 EXPERIMENTAL DETAILS:

5.2.1 Ring Compression Test:

5.2.2: Compression Test of Composites:

5.3 RESULTS AND DISCUSSION:

5.3.1 Compressive Behavior:

Compressive properties of the alloy and composites have been studied from the load-displacement curves. Figure 5.6 and 5.7 shows the true stress–true strain curves of alloy and composites with aspect ratios of 1.0 and 1.5 respectively. This was treated to be material property and used as input for finite element analysis discussed in chapter 6.

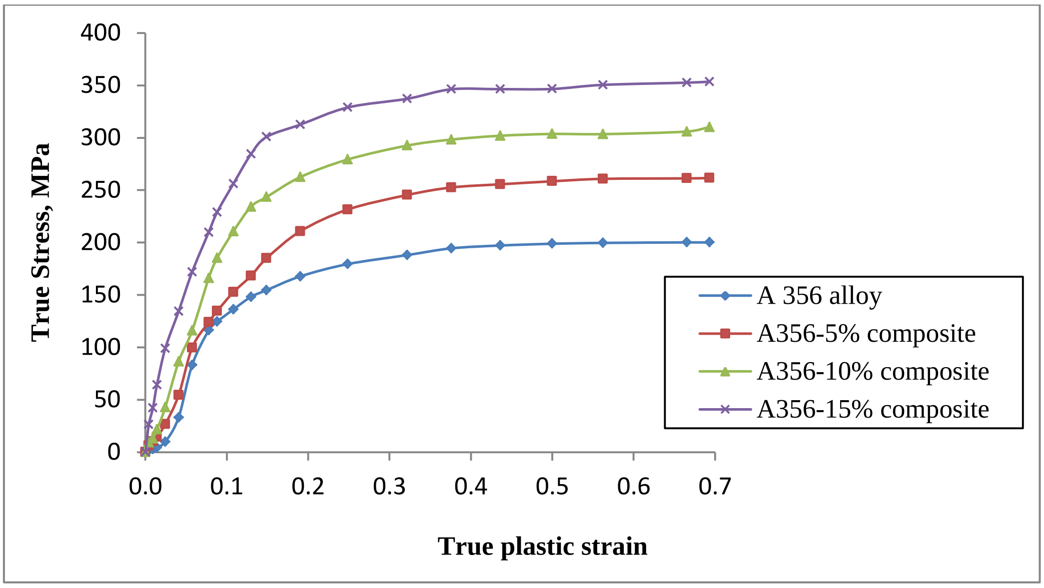

Figure 5.6 True stress vs true plastic strain for Ho/Do =1.0

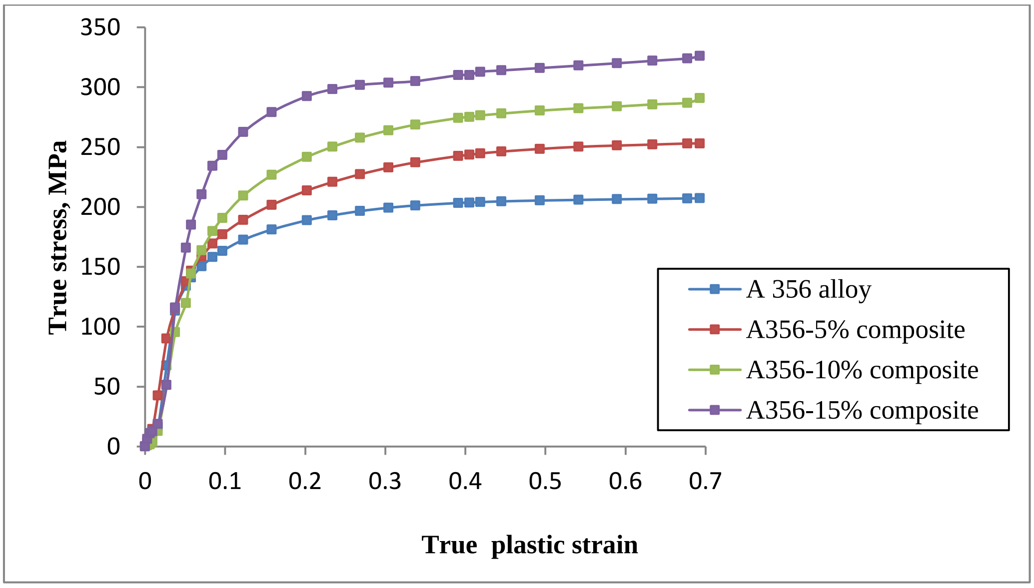

Figure 5.7 True stress vs True plastic strain for Ho/Do =1.5

5.3.2 Hollomon Power Law Parameters

$= K \bar{\varepsilon}^{n}$ ---------- (5.9) $\bar{\sigma}$

5.4 CONCLUSIONS:

1. Strength coefficient increased with increase in reinforcement content compared to the alloy.

2. At high aspect ratio both alloy and the composites exhibit lower compression strength values.

3. Strain hardening exponent increased with increase in reinforcement content compared to the alloy.

4. At high aspect ratio, strength coefficient decreased while strain hardening exponent increased.

5. For both alloy and composites effective strain increased and the circumferential stress component become tensile with continued deformation.

6. The increase in circumferential stress component value was found to be more in case of specimens deformed for lower aspect ratio compared to the higher aspect ratio conditions.

7. The axial stresses, for alloy as well as the composites increased in the very initial stages of deformation but started becoming less compressive immediately as barreling developed.

8. At the beginning of deformation axial compressive stress increased in magnitude but as the deformation progress the magnitude reduced.

9. Hydrostatic stress is reduced in magnitude as the deformation increased.

VI. FINITE ELEMENT SIMULATION OF COLD UPSETTING PROCESS

6.1 INTRODUCTION:

The upsetting of solid cylinders is an important metal forming process and an important stage in the forging sequence of many products. Cold forming process minimizes material wastage, improves mechanical properties such as yield strength and hardness and provides very good surface finish. The tools used are also subjected less thermal fatigue [9]. Metal flow is influenced mainly by various parameters like specimen geometry, friction conditions, characteristics of the stock material, thermal conditions existing in the deformation zone, and strain rate. Metal flow influence the quality and the properties of the formed product; the force and energy requirements of the process. A large segment of industry depends primarily on the predominant applications of this process which includes coining, heading and closed die forming.

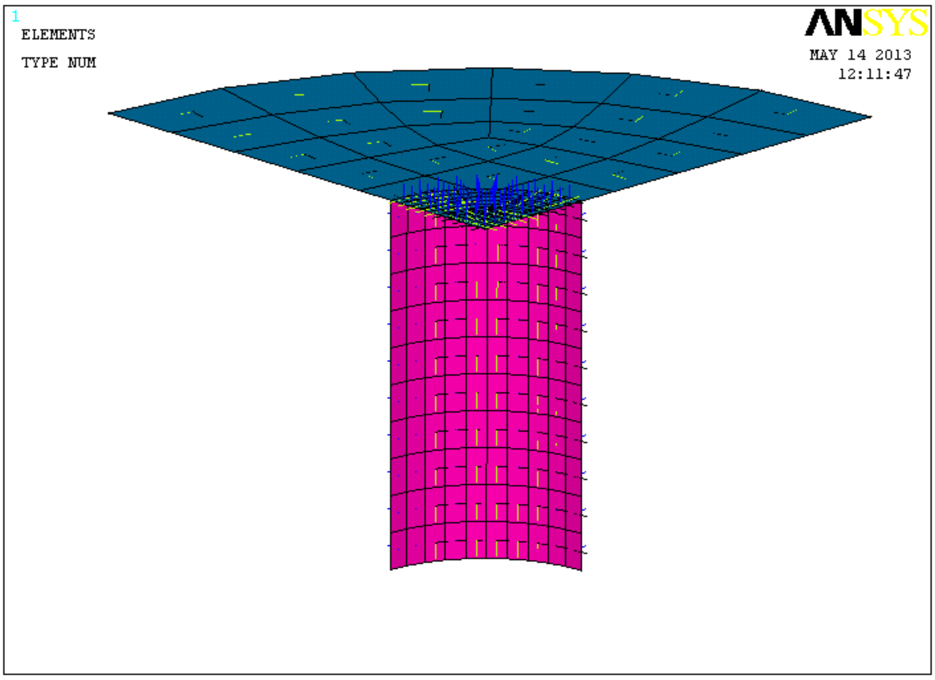

Figure 6.2: Contact pair between die and composite model

6.1.2 Material Properties and Real Constants:

The material models selected were based on the properties of the tooling and billet materials. Due to high structural rigidity of the tooling, only the following elastic properties of tooling (H13 steel) were assigned assuming the material to be isotropic [10].

Young’s Modulus E = 220 GPa (for steel)

International Journal of Mechanical and Industrial Technology ISSN 2348-7593 (Online)
Vol. 3, Issue 1, pp: (269-281), Month: April 2015 - September 2015, Available at: www.researchpublish.com

Poisson's ratio υ = 0.3

6.2 RESULTS AND DISCUSSION:

Figure 6.3 and 6.4 shows the meshed models of billets and tooling for the aspect ratios of 1.0 and 1.5 respectively. Figure 6.5 and 6.6 shows the 50% deformation specimen with zero friction for the aspect ratios of 1.0 and 1.5 respectively. Since there was no friction at metal-die contact, the deformation can be treated as homogeneous since no bulging was seen. The maximum radial displacement corresponding to 50% for the aspect ratio of 1.0 is shown as 2.435mm in figure 6.7. This means that the diameter after 50% deformation equals to 12 + 2 X 2.435 = 16.87 mm. The value of analytically determined diameter after 50% equals to 12 X $\sqrt{2}$ = 16.970 mm, (assuming volume constancy) leading to a very little error of 0.59% usually can be discarded in non-linear finite element analysis such as in large deformation / metal forming applications.

For the present study the friction factor 'm' was found to be 0.36 (explained in page 94, chapter 5) and the extent of barreling with this friction at 50% deformation for alloy and composites under investigation was shown in figures 6.9-6.40 respectively. Similar results on finding the friction were observed by many authors [11-28]. Lower aspect ratio (H_0/D_0 = 1.0) samples has shown more barreling affect compare to higher aspect ratio (H_0/D_0 = 1.5). The above results were experimentally evidenced, as discussed in chapter 5.

The notations used in the analysis were, radial displacements (UX): circumferential stress, σ_θ (SY), axial stress σ_z (SZ), hydrostatic stress, σ_H (NLHPRE), Von-Mises equivalent stress $\bar{\sigma}$ (SEQV).

The variations in FEA results compared to analytical results obtained in chapter 5 were shown in figures 6.45 to 6.48. The obtained FEA results revealed that these values are closely matching with the experimental values. Hence the FEA model adopted for solving the present upsetting analysis was validated with the analytical results of chapter 5.

A square shaped billet was taken and tested by applying the same material properties, and validated the results, as shown in figures 6.41-6.44, the platens were considered as rigid and due to symmetry, half portion was taken for analysis to reduce the problem size.

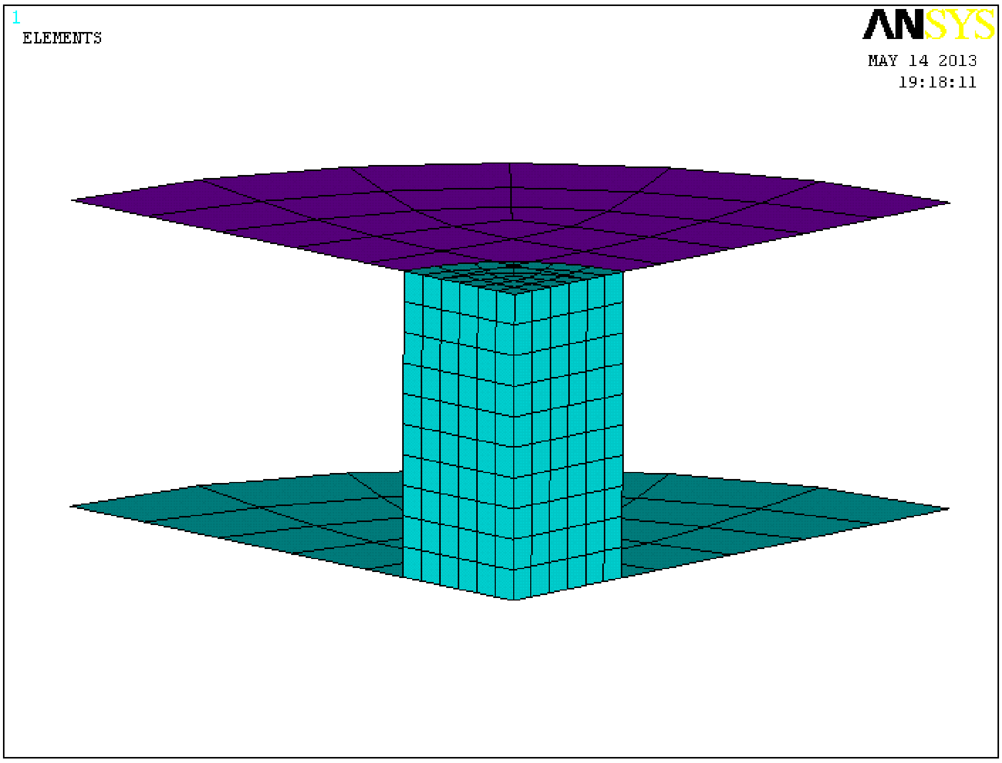

Figure 6.3: Undeformed sample (H_0/D_0 = 1.0)

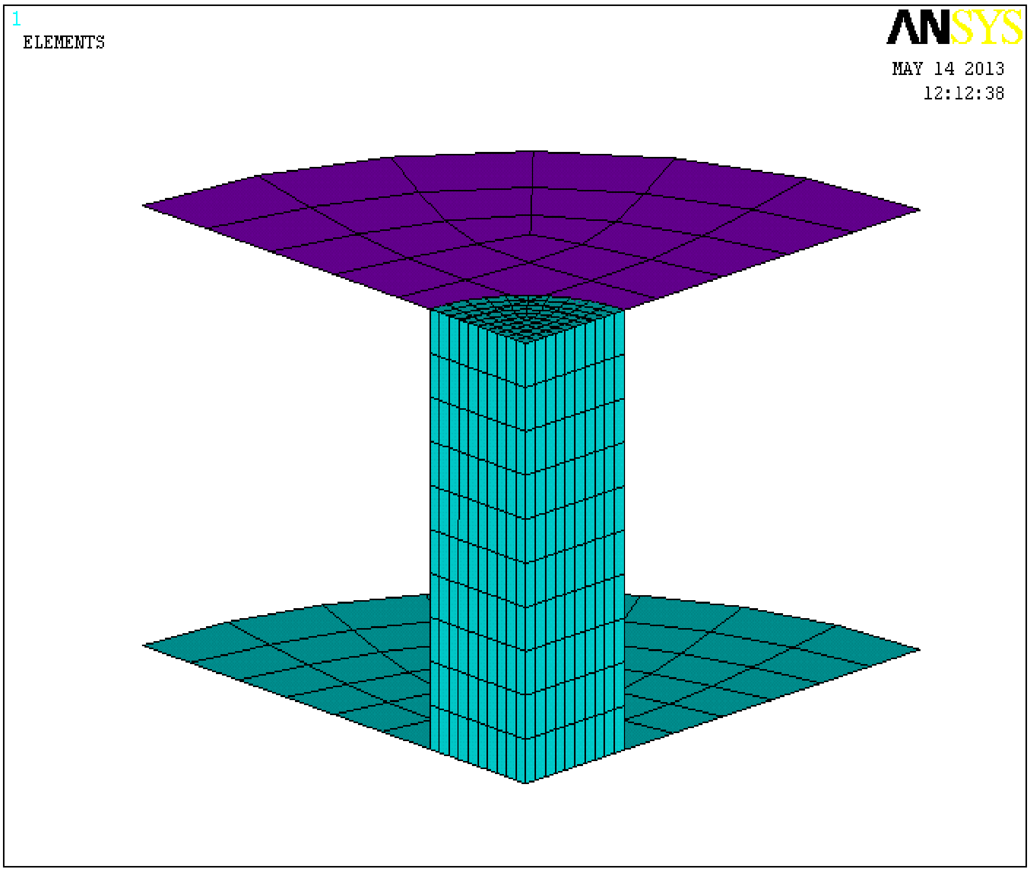

Figure 6.4: Unreformed sample (H_0/D_0 = 1.5)

VII. CONCLUSIONS

Detailed comparisons of the experimental variables with the finite element method (FEM) results were carried out to ascertain the accuracy with which the deformation process can be modelled. Predictions from the simulation results were found to be in good agreement with the actual experimentation.

1. Finite element analysis of deformation behaviour of cold upsetting process was carried out for all the $HSA_{(P)}$ composites and base alloy (A356) with aspect ratios of 1.0 and 1.5 in dry condition.
2. Due to axisymmetric nature of the geometry only quarter portion was modeled with symmetric boundary conditions.
3. Rigid-flexible contact analysis was performed for the forming process, so that the die appears like a thin plate, and the stress analysis was done on the billet only.
4. FEM analysis, need material characteristics of composites. The stress strain curve obtained through UTM was only used for the analysis. The material models used in ansys helped in better correlation with results.
5. Once the material properties for composites and material model to be selected from ansys are finalised, the future designs that are going to be produced through these composites will require less time for manufacture.
6. The accuracy of results depends on the accuracy of the input data (true stress-true strain behaviour and friction factor obtained from the experiments) and friction model used in the analysis.

ACKNOWLEDGEMENT

I have received generous help from a number of people to carry on my research work. Without their co-operation and encouragement I could not have completed my work. With pleasure I acknowledge my irredeemable debt to them. I am very much thankful to my parents for their encouragement and support for the completion of the present project work.

REFERENCES

[1] M. Surappa, Aluminium matrix composites: Challenges and opportunities, Vol 28, Parts 1&2, February/April 2003, pp 319-334.

[2] D.B. Miracle and S.L. Donaldson, Air force research laboratory, pp 1-2.

[3] T.W.Clyne, An Introductory overview of MMC system, types and developments, in comprehensive composite materials, Vol-3; Metal matrix composites, Elsevier, 2000, pp.1-26.

[4] N. Bowler and Y. Huang, Electrical conductivity measurements of metal plates using broad band eddy-current and four-point methods, Meas. Sci. Technol. 16, 2005, pp. 2193-2200.

[5] L.F. Mondolfo, Aluminium alloy: Structure and properties, Butterworth and Co ltd, London, (1976) 253.

[6] X. Yang, J.D. Hunt and D.V. Edmonds, Aluminium alloys, 69(2), 1993, p.158.

[7] B. Zlaticanin, Characterization of microstructure and properties of Al-Cu-Mg alloy, Journal of mining and metallurgy, Vol 39, 2003, pp. 509-526.

[8] M. Rout, Flow stress and barreling behavior of aluminum alloy solid cylinder during upset forging at elevated temperature, NIT Rourkela 2011.

[9] M. Jolgaf, A.M.S Hamouda, S. Suleiman and M.M. Hamdan 2003, Development of a CAD/CAM system for the closed–die forging process, Journal of Material Processing Technology, 138: pp.436-442.

[10] http://www.matweb.com.